

Journal Pre-proof



Macrophage Scavenger Receptor 1 mediates lipid-induced inflammation in non-alcoholic fatty liver disease

Olivier Govaere, Sine Kragh Petersen, Nuria Martinez-Lopez, Jasper Wouters, Matthias Van Haele, Rosellina M. Mancina, Oveis Jamialahmadi, Orsolya Bilkei-Gorzo, Pierre Bel Lassen, Rebecca Darlay, Julien Peltier, Jeremy M. Palmer, Ramy Younes, Dina Tiniakos, Guruprasad P. Aithal, Michael Allison, Michele Vacca, Melker Göransson, Rolando Berlinguer-Palmini, James E. Clark, Michael J. Drinnan, Hannele Yki-Järvinen, Jean-Francois Dufour, Mattias Ekstedt, Sven Francque, Salvatore Petta, Elisabetta Bugianesi, Jörn M. Schattenberg, Christopher P. Day, Heather J. Cordell, Baki Topal, Karine Clément, Stefano Romeo, Vlad Ratziu, Tania Roskams, Ann K. Daly, Quentin M. Anstee, Matthias Trost, Anetta Härtlova

PII: S0168-8278(21)02254-6

DOI: <https://doi.org/10.1016/j.jhep.2021.12.012>

Reference: JHEPAT 8540

To appear in: *Journal of Hepatology*

Received Date: 26 March 2021

Revised Date: 5 December 2021

Accepted Date: 7 December 2021

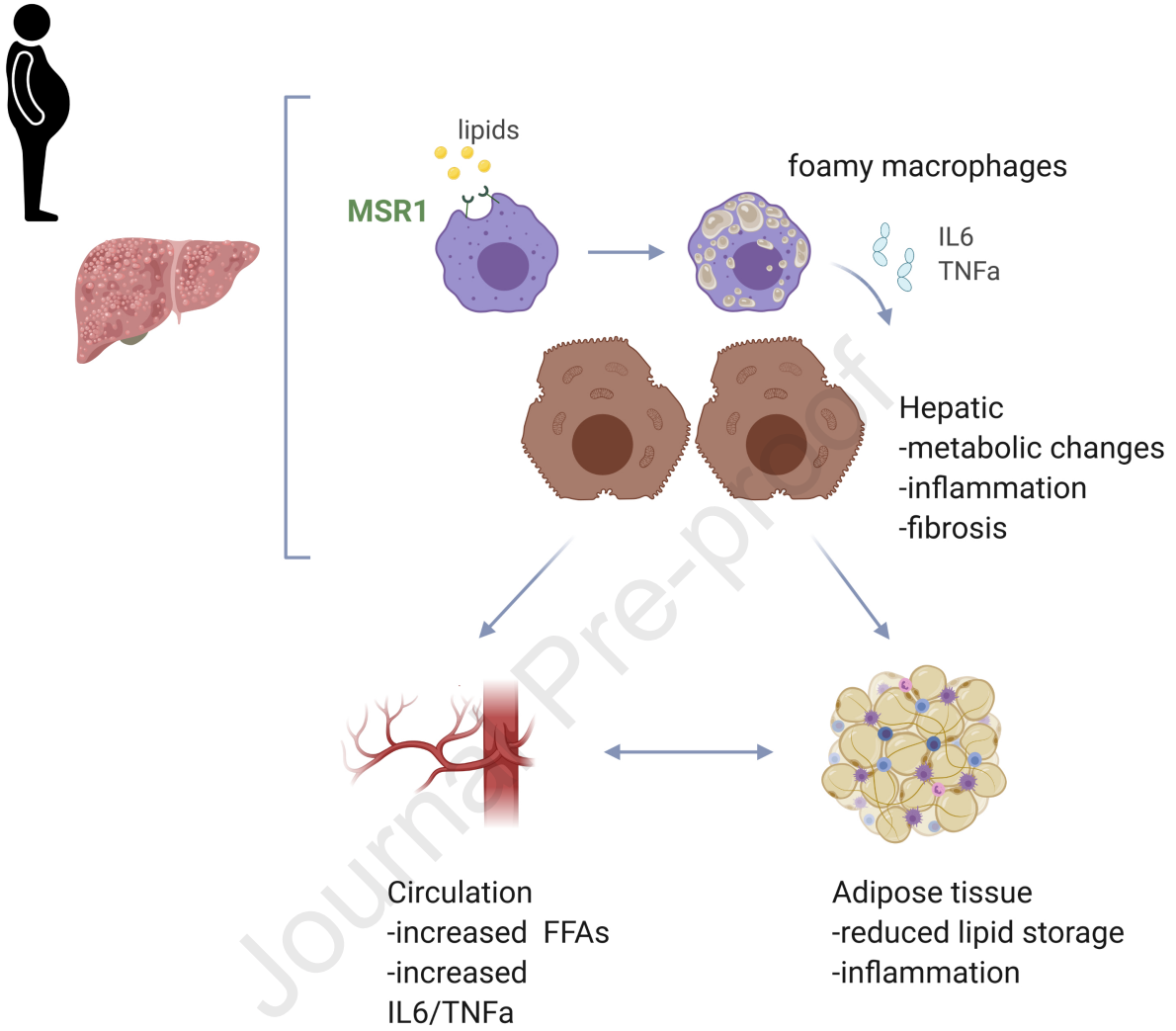
Please cite this article as: Govaere O, Petersen SK, Martinez-Lopez N, Wouters J, Van Haele M, Mancina RM, Jamialahmadi O, Bilkei-Gorzo O, Lassen PB, Darlay R, Peltier J, Palmer JM, Younes R, Tiniakos D, Aithal GP, Allison M, Vacca M, Göransson M, Berlinguer-Palmini R, Clark JE, Drinnan MJ, Yki-Järvinen H, Dufour JF, Ekstedt M, Francque S, Petta S, Bugianesi E, Schattenberg JM, Day CP, Cordell HJ, Topal B, Clément K, Romeo S, Ratziu V, Roskams T, Daly AK, Anstee QM, Trost M, Härtlova A, Macrophage Scavenger Receptor 1 mediates lipid-induced inflammation in non-alcoholic fatty liver disease, *Journal of Hepatology* (2022), doi: <https://doi.org/10.1016/j.jhep.2021.12.012>.

This is a PDF file of an article that has undergone enhancements after acceptance, such as the addition of a cover page and metadata, and formatting for readability, but it is not yet the definitive version of record. This version will undergo additional copyediting, typesetting and review before it is published in its final form, but we are providing this version to give early visibility of the article. Please note that,

during the production process, errors may be discovered which could affect the content, and all legal disclaimers that apply to the journal pertain.

© 2021 Published by Elsevier B.V. on behalf of European Association for the Study of the Liver.

Non-alcoholic fatty liver disease



1 **Macrophage Scavenger Receptor 1 mediates lipid-induced inflammation in non-alcoholic fatty liver**
2 **disease**

3
4 Olivier Govaere^{1*†}, Sine Kragh Petersen^{2‡}, Nuria Martinez-Lopez^{3,4‡}, Jasper Wouters^{5,6}, Matthias Van
5 Haele⁷, Rosellina M. Mancina⁸, Oveis Jamialahmadi⁸, Orsolya Bilkei-Gorzo², Pierre Bel Lassen⁹, Rebecca
6 Darlay¹⁰, Julien Peltier¹¹, Jeremy M. Palmer¹, Ramy Younes^{1,12}, Dina Tiniakos^{1,13}, Guruprasad P. Aithal¹⁴,
7 Michael Allison¹⁵, Michele Vacca¹⁶, Melker Göransson¹⁷, Rolando Berlinguer-Palmini¹⁸, James E. Clark¹,
8 Michael J Drinnan¹, Hannele Yki-Järvinen¹⁹, Jean-Francois Dufour^{20,21}, Mattias Ekstedt²², Sven Francque²³,
9 Salvatore Petta²⁴, Elisabetta Bugianesi¹², Jörn M Schattenberg²⁵, Christopher P. Day¹, Heather J. Cordell¹⁰,
10 Baki Topal²⁶, Karine Clément⁹, Stefano Romeo⁸, Vlad Ratziu²⁷, Tania Roskams⁷, Ann K. Daly¹, Quentin M.
11 Anstee^{1,28*†}, Matthias Trost^{11*†}, Anetta Härtlova^{2,11*†}

12
13 **Affiliations:**

14 ¹Translational and Clinical Research Institute, Faculty of Medical Sciences, Newcastle University,
15 Newcastle upon Tyne, United Kingdom.

16 ²Wallenberg Centre for Molecular and Translational Medicine, Department of Microbiology and
17 Immunology at Institute of Biomedicine, University of Gothenburg, Gothenburg, Sweden.

18 ³Department of Medicine, Albert Einstein College of Medicine, Bronx, NY 10461, USA

19 ⁴Department of Radiation Oncology, Albert Einstein College of Medicine, Bronx, NY 10461, USA

20 ⁵Center for Brain & Disease Research, VIB-KU Leuven, Leuven, Belgium

21 ⁶Department of Human Genetics, KU Leuven, Leuven, Belgium

22 ⁷Department of Imaging and Pathology, Translational Cell and Tissue Research, KU Leuven and University
23 Hospitals Leuven, Leuven, Belgium

24 ⁸The Wallenberg Laboratory for Cardiovascular and Metabolic Research, Department of Molecular and
25 Clinical Medicine, University of Gothenburg, Gothenburg, Sweden.

26 ⁹Nutrition and obesity: systemic approaches, Inserm, Sorbonne University, Paris, France.

27 ¹⁰Population Health Sciences Institute, Faculty of Medical Sciences, Newcastle University, Newcastle upon
28 Tyne, United Kingdom.

29 ¹¹Biosciences Institute, Faculty of Medical Sciences, Newcastle University, Newcastle upon Tyne, United
30 Kingdom.

31 ¹²Department of Medical Sciences, Division of Gastro-Hepatology, A.O. Città della Salute e della Scienza di
32 Torino, University of Turin, Turin, Italy.

33 ¹³Department of Pathology, Aretaieio Hospital, National & Kapodistrian University of Athens, Athens,
34 Greece.

35 ¹⁴NIHR Nottingham Biomedical Research Centre, Nottingham University Hospitals NHS Trust and
36 University of Nottingham, Nottingham, United Kingdom.

37 ¹⁵Liver Unit, Department of Medicine, Cambridge NIHR Biomedical Research Centre, Cambridge University
38 NHS Foundation Trust, United Kingdom.

39 ¹⁶University of Cambridge Metabolic Research Laboratories, Wellcome-MRC Institute of Metabolic
40 Science, Addenbrooke's Hospital, Cambridge, United Kingdom.

41 ¹⁷Bioscience COPD/IPF, Research and Early Development, Respiratory and Immunology (R&I),
42 BioPharmaceuticals R&D, AstraZeneca, Gothenburg, Sweden.

43 ¹⁸Bioimaging Unit, Faculty of Medical Sciences, Newcastle University, Newcastle upon Tyne, United
44 Kingdom.

45 ¹⁹Minerva Foundation Institute for Medical Research and Department of Medicine, University of Helsinki,
46 Helsinki, Finland.

47 ²⁰University Clinic for Visceral Surgery and Medicine, University of Bern, Bern, Switzerland.

48 ²¹Hepatology, Department of Biomedical Research, University of Bern, Bern, Switzerland

49 ²²Division of Gastroenterology and Hepatology, Department of Medicine and Health Sciences, Linköping
50 University, Linköping, Sweden.

51 ²³Department of Gastroenterology and Hepatology, Antwerp University Hospital & University of Antwerp,
52 Antwerp, Belgium.

53 ²⁴Sezione di Gastroenterologia, Dipartimento Biomedico di Medicina Interna e Specialistica, Università di
54 Palermo, Palermo, Italy.

55 ²⁵I. Department of Medicine, University Hospital Mainz, Mainz, Germany.

56 ²⁶Department of Abdominal Surgery, KU Leuven and University Hospitals Leuven, Leuven, Belgium

57 ²⁷Assistance Publique-Hôpitaux de Paris, hôpital Beaujon, University Paris-Diderot, Paris, France.

58 ²⁸Newcastle NIHR Biomedical Research Centre, Newcastle upon Tyne Hospitals NHS Trust, Newcastle
59 upon Tyne, United Kingdom.

60

61 †Senior authors ‡ contributed equally *Corresponding authors

62 **Correspondence:**

63 Dr. Olivier Govaere, PhD

64 Translational and Clinical Research Institute,

65 The Medical School, Newcastle University,

66 4th Floor, William Leech Building,

67 Framlington Place, Newcastle-upon-Tyne, NE2 4HH, United Kingdom

68 Email: olivier.govaere@newcastle.ac.uk

69

70 Dr Anetta S. Härtlova, PhD

71 Assistant Professor

72 Wallenberg Centre for Molecular and Translational Medicine

73 University of Gothenburg, Institute of Biomedicine

74 Department of Microbiology and Immunology

75 Medicinaregatan 7 A, 40530 Göteborg, Sweden

76 Email: anetta.hartlova@gu.se

77

78 Prof Matthias Trost, PhD

79 Biosciences Institute,

80 The Medical School, Newcastle University,

81 4th Floor, William Leech Building,

82 Framlington Place, Newcastle-upon-Tyne, NE2 4HH, United Kingdom

83 Email:matthias.trost@newcastle.ac.uk

84

85 Prof Quentin M. Anstee, PhD, FRCP

86 Translational and Clinical Research Institute,

87 The Medical School, Newcastle University,

88 4th Floor, William Leech Building,

89 Framlington Place, Newcastle-upon-Tyne, NE2 4HH, United Kingdom

90 Email: quentin.anstee@newcastle.ac.uk

91

92 **Key words:** macrophages, immunometabolism, NASH, inflammation

93 **Word counts:** 6,098 (including abstract, references, table, figure legends)

94 **Number of figures and tables:** 6 figures and 1 table

95 **Conflict of interest:** The authors have no potential conflicts (financial, professional or personal) directly
96 relevant to the manuscript.

97 **Funding:** This study has been supported by the EPOS (Elucidating Pathways of Steatohepatitis)
98 consortium funded by the Horizon 2020 Framework Program of the European Union under Grant
99 Agreement 634413, the LITMUS (Liver Investigation: Testing Marker Utility in Steatohepatitis)
100 consortium funded by the Innovative Medicines Initiative (IMI2) Program of the European Union under
101 Grant Agreement 777377, which receives funding from the EU Horizon 2020 programme and EFPIA, and
102 the Newcastle NIHR Biomedical Research Centre (to QMA), the Newcastle University start-up funding
103 and the Wellcome Trust Investigator Award (215542/Z/19/Z) (to MT), Knut och Alice Wallenberg
104 Foundation Wallenberg Centre for molecular and translational medicine, University of Gothenburg,
105 Sweden and Åke Wirbergs Research funding #M18-0121 (to AH), Cancerfonfen # 19 0352 Pj (2020-2022)
106 (to AH), the Belgian Federal Science Policy Office (Interuniversity Attraction Poles Program) grant
107 Network P7/83-HEPRO2 (to TR), Rosetrees Trust (to NML), Flemish Cancer Society Kom op tegen Kanker,
108 and Belgian Cancer Society Stichting tegen Kanker (to J.W).

109 **Author contributions:** OG and AH conceived the study. Study design, manuscript drafting and funding:
110 AH, OG, MT and QMA. Manuscript preparation: AH, OG, SKP, MT, QMA. *In vivo* experiments: AH, SKP,
111 OBG and NML. *In vitro* experiments: AH, OG and SKP. Human *ex vivo* experiments: OG, MVH, TR.
112 Histopathology: OG, MVH, TR and DT. Nanostring analysis: OG. Bioinformatics: OG and JW. GWAS
113 analysis: RD, HJC, AKD. eQTL UKBiobank data: RMM, OJ, SR. All authors contributed to data collection
114 and interpretation, and critically revised the manuscript for intellectual content.

115 **Data and materials availability:**

116 To review GEO accession GSE163471:

117 Go to <https://www.ncbi.nlm.nih.gov/geo/query/acc.cgi?acc=GSE163471>

118 Enter token khehmemolruhbcj into the box

119

120

121 **Lay summary**

122 Non-alcoholic fatty liver disease (NAFLD) is a chronic disease primarily caused by excessive consumption
123 of fat and sugar combined with a lack of exercise or a sedentary life style. Here we show that the
124 macrophage scavenger receptor MSR1, an innate immune receptor, mediates lipid uptake and
125 accumulation in Kupffer cells resulting in liver inflammation, and thereby promoting the progression of
126 NAFLD in human and in mice.

Journal Pre-proof

127 **Abstract:**

128 Background & Aims: Obesity-associated inflammation is a key player in the pathogenesis of non-
129 alcoholic fatty liver disease (NAFLD). However, the role of macrophage scavenger receptor 1 (MSR1,
130 CD204) remains incompletely understood.

131 Methods: 170 NAFLD liver biopsies were processed for transcriptomic analysis and correlated with
132 clinicopathological features. *Msr1*^{-/-} and WT mice were submitted to a 16 week high-fat and high-
133 cholesterol diet. Therapeutic intervention with monoclonal antibody against MSR1 was performed in
134 mice and *ex vivo* human liver slices. Genetic susceptibility was assessed using GWAS data from 1,483
135 NAFLD patients and 430,101 participants of the UKBiobank.

136 Results: MSR1 expression was associated with the occurrence of hepatic lipid-laden foamy macrophages
137 and correlated with the degree of steatosis and steatohepatitis in NAFLD patients. Mice lacking *Msr1*
138 were protected against diet-induced metabolic disorder, showing fewer hepatic foamy macrophages,
139 less hepatic inflammation, improved dyslipidemia and glucose tolerance, while showing altered hepatic
140 lipid metabolism. MSR1 induced a pro-inflammatory response via the JNK signalling pathway upon
141 triggering by saturated fatty acids. *In vitro* blockade of the receptor prevented the accumulation of lipids
142 in primary macrophages which inhibited the switch towards a pro-inflammatory phenotype and the
143 release of cytokines such as TNF- α . Targeting MSR1 using monoclonal antibody therapy in an obesity-
144 associated NAFLD mouse model and human liver slices resulted in the prevention of foamy macrophage
145 formation and inflammation. Moreover, we identified that rs41505344, a polymorphism in the upstream
146 transcriptional region of *MSR1*, was associated with altered serum triglycerides and aspartate
147 transaminase levels in a cohort of over 400,000 patients.

148 Conclusions: Taken together, our data suggest a critical role for MSR1 in lipid-induced inflammation and
149 a potential therapeutic target for the treatment of NAFLD.

150

151 Introduction

152 With the increasing prevalence of obesity, non-alcoholic fatty liver disease (NAFLD) has become the
153 most common chronic liver disease globally.¹ NAFLD is characterised by excessive hepatic triglyceride
154 accumulation and represents a series of diseased states ranging from isolated steatosis (non-alcoholic
155 fatty liver, NAFL) to non-alcoholic steatohepatitis (NASH), identified by the presence of necro-
156 inflammation and hepatocyte ballooning, with varying degrees of fibrosis. NAFLD is strongly linked with
157 metabolic syndrome, i.e. dyslipidemia, hypertension, obesity and type 2 diabetes mellitus (T2DM), and
158 currently affects 20 to 30% of the global population.¹ Importantly, not all patients progress from NAFL to
159 NASH and although gene signatures of more advanced fibrosing-steatohepatitis have been identified,
160 the exact pathogenic pathways involved in the initiating phases of the disease, especially the transition
161 from NAFL to NASH, are not fully understood.²

162
163 Growing evidence supports the view that Kupffer cells, the endogenous hepatic macrophages, are
164 initiators of inflammation and hence contribute to NAFLD development, whilst recruited monocyte-
165 derived macrophages are often observed in advanced stages of the disease.³ Hepatic macrophages are
166 responsive to a variety of stimuli including bacterial endotoxins (such as lipopolysaccharide) but also
167 free fatty acids (FFAs) or cholesterol.⁴ Excess of FFAs and cholesterol can cause the formation of hepatic
168 foamy macrophages, and leads to Kupffer cell aggregates and lipogranulomas during steatohepatitis.⁵
169 Specifically, the intake of saturated fat has been shown to induce insulin resistance, and to enhance
170 intrahepatic triglyceride accumulation and steatohepatitis.⁶

171 Palmitic acid (PA), rather than non-saturated fatty acids (non-SFA), has been shown to be a strong
172 inducer of inflammation in immortalised cell lines through activation of the downstream JNK signalling
173 pathway.⁷ Recent data show that pro-inflammatory activation of murine bone marrow-derived
174 macrophages by PA is independent of Toll-like receptor 4, yet the receptor that is responsible is still not
175 known.⁸ Recently, we have shown that *in vitro* activation of the phagocytic receptor, macrophage
176 scavenger receptor 1 (MSR1, also known as SR-A or CD204), results in pro-inflammatory macrophage
177 polarisation through JNK activation.⁹ MSR1 is a key macrophage receptor for the clearance of circulating
178 lipoproteins and has been implicated in atherogenesis.¹⁰ In irradiated low-density lipoprotein receptor-
179 deficient mice, transplantation of *Msr1*^{-/-}/*CD36*^{-/-} monocytes proved to reduce dietary-induced
180 inflammation.¹¹ However, the molecular mechanisms underlying hepatic macrophage activation and/or
181 the formation of foamy macrophages in NAFLD remain poorly understood. We therefore hypothesised

182 that MSR1 might be involved in inflammatory responses in the context of lipid overload during obesity-
183 induced NAFLD.

184

185 **Materials and Methods**

186 **Patient selection**

187 Cases were derived from the European NAFLD Registry (NCT04442334), approved by the relevant Ethical
188 Committees in the participating centres, and all patients having provided informed consent.¹² For the
189 histopathological and nanoString® study, 194 formalin-fixed paraffin-embedded (FFPE) or frozen liver
190 biopsies samples were obtained from patients diagnosed with histological proven NAFLD at the Freeman
191 Hospital, Newcastle Hospitals NHS Foundation Trust, Newcastle-upon-Tyne, UK and at the Pitié-
192 Salpêtrière Hospital, Paris, France (**Table S1**). For the Genome Wide Association Study, 1,483 patients
193 with histological proven NAFLD were included as previously described.¹³ All liver tissue samples for the
194 histopathological and nanoString® study were centrally scored according to the semi-quantitative NASH-
195 CRN Scoring System by an expert liver pathologist (DT).¹⁴ Fibrosis was staged from F0 through to F4
196 (cirrhosis). Alternate diagnoses and etiologies such as excessive alcohol intake, viral hepatitis,
197 autoimmune liver diseases and steatogenic medication use were excluded. Viable human normal liver
198 tissue for the *ex vivo* slices was obtained after resection from two adult patients treated at the
199 University Hospitals Leuven, Leuven, Belgium. Samples were assessed by an expert liver pathologist (TR).

200 **Animals**

201 Male *Msr1*^{-/-} or *Msr1*^{+/+} (wild type, WT) C57BL/6 mice were either kindly provided by Prof. Siamon
202 Gordon, University of Oxford or obtained from Jackson Laboratories and bred in a conventional animal
203 facility under standard conditions. Animals received human care and experimental protocols were
204 approved by the institutional animal ethics committees at Newcastle University (PC123A338) and
205 University of Gothenburg (2947/20). Mice had free access to water and were fed either standard chow
206 (n=10, 5 WT and 5 *Msr1*^{-/-}) or 45%-high-fat and high-cholesterol diets (HFD; 820263, Special Diet
207 Services; n=10, 5 WT and 5 *Msr1*^{-/-}) ad libitum. For the therapeutic intervention, WT mice were put on a
208 12 week HFD and intravenously injected with monoclonal rat anti-mouse *Msr1* antibody (n=8 animals,
209 MAB1797-SP, R&Dsystems) or IgG control (n=9 animals, MAB0061, R&D systems) at week 10 and 11
210 (0.25 mg antibody/animal).

211

212 **Statistical analysis**

213 Kolmogorov-Smirnov or the Shapiro-Wilk normality test, unpaired Student's t-test or Mann-Whitney U
214 test, one way ANOVA or Kruskal-Wallis test with respectively Tuckey's or Dunn's post hoc multiple
215 comparison test or Chi-Square test were performed using IBM SPSS statistics 26 or GraphPad Prism
216 8.4.3. A p-value<0.05 was considered significant. Binary logistic regression analysis was performed in
217 SPSS using Backward Stepwise Likelihood Ratio model. The model predicting high disease activity $NAS \geq 4$
218 was calculated as follows: $MSR1_model = -1.296883 + (0.003020 * MSR1_mRNA)$.

219

220 *Additional Material and Methods can be found in the Supplementary Materials.*

221

222 **Results**

223 *MSR1 expression correlates with steatohepatitis activity in human NAFLD*

224 To investigate the role of MSR1 in human NAFLD, we first analysed gene expression in a cohort of 170
225 histologically characterised human adult liver biopsies. The cohort was stratified according to
226 histopathological disease grade and stage, i.e. NAFL and NASH with fibrosis ranging from F0 to F4 (**Table**
227 **S1**). Univariate analysis indicated that *MSR1* transcript was significantly associated with high steatosis,
228 hepatocyte ballooning, lobular inflammation, presence of NASH and a NAFLD Activity Score ≥ 4 (NAS,
229 defined as the sum of steatosis, ballooning and lobular inflammation) (**Fig.1a-b** and **Table S2**).¹⁴

230 Interestingly, *CD68* mRNA, a marker for monocytes/macrophages, was only significantly associated with
231 $NAS \geq 4$ but not with any other clinicopathological features (**Table S2**). To further explore whether *MSR1*
232 transcript was independently associated with high disease activity, we performed binary logistic
233 regression analysis including the clinical variables sex, body mass index (BMI), age, T2DM, alanine
234 aminotransferase (ALT) and aspartate aminotransferase (AST), together with *MSR1* and *CD68* mRNA
235 levels. Backward Stepwise Likelihood Ratio modelling showed that *MSR1* transcript levels predicted
236 $NAS \geq 4$ independently from *CD68* mRNA or other clinical variables with an Area Under the Curve of 0.735
237 (**Fig.1c**).

238 Histopathological analysis showed that MSR1 was predominantly expressed in resident liver
239 macrophages, the Kupffer cells, rather than infiltrating monocyte-derived macrophages located in the
240 portal tract, as visualised by the MSR1 and CD68 immunostaining (**Fig.1d** and **Fig.S1a-b**). This was
241 confirmed by immunofluorescent double staining (**Fig.S1c**). While the number of infiltrating portal CD68-
242 immunopositive cells increased with disease progression ($p < 0.05$), no significant differences were found

243 for infiltrating MSR1-positive cells (**Fig.1d**). These results were supported by publicly available single cell
244 RNA sequencing data indicating that *MSR1* expression was mainly restricted to the Kupffer cell
245 population whereas *CD68* was also expressed in monocyte populations (**Fig.S2a-b**).¹⁵ Moreover, when
246 differentiating monocytes from healthy individuals towards mature macrophages, we observed an
247 increase in MSR1 protein expression (**Fig.1e**). Notably, MSR1 immunopositivity was also seen in
248 lipogranulomas and lipid laden macrophages throughout the spectrum of NAFLD (**Fig.1d and Fig.S1a**).
249 Using the marker Perilipin 2 (PLIN2) to visualise intracellular lipid droplets, immunofluorescence analysis
250 showed that lipid droplets accumulate in the Kupffer cells (**Fig.1f**). Furthermore, a significant increase in
251 parenchymal CD68+_PLIN2+ cells was observed in NAFLD patients stratified based on NAS \geq 4 or steatosis
252 grade \geq 2 (**Fig.1f**).

253 Taken together, these human data demonstrate a positive correlation of *MSR1* transcript and protein
254 levels with NAFLD disease activity and the occurrence of hepatic-resident lipid-laden macrophages in the
255 presence of excessive lipids.

256

257 *Msr1* deficiency protects against diet-induced metabolic dysregulation and liver damage in mice

258 To further investigate how MSR1 functionally contributes to the development of obesity-related NAFLD,
259 we subjected *Msr1*^{-/-} mice (n=5) and their corresponding *Msr1*^{+/+} (n=5 WT) age-matched male
260 counterparts to a high-fat and high-cholesterol diet (HFD) for 16 weeks. Upon HFD feeding, *Msr1*-
261 deficient mice displayed increased total body weight, an increase in liver and epididymal white adipose
262 tissue (eWAT) weight and increased food intake compared to WT (**Fig.2a-b, Fig S3a-b**). Furthermore,
263 HFD-fed *Msr1*^{-/-} mice exhibited improved glucose uptake from blood, higher serum leptin, lower
264 concentrations of circulating FFAs and enhanced fatty acid accumulation in the adipocytes (**Fig.2c,**
265 **FigS3c-d**). Consistently the adipocytes in HFD-fed *Msr1*^{-/-} mice were larger compared to WT, suggesting
266 an increased adiposity and fat storage in the absence of *Msr1* (**Fig.2d-e**). Although no murine models
267 accurately recapitulate all histological features of human steatohepatitis, histological and transcriptomic
268 features of liver fibrosis were clearly attenuated by *Msr1* deficiency upon HFD feeding (**Fig.2d-f**). Sixteen
269 weeks of regular diet did not result in any histological differences between the livers of WT and *Msr1*^{-/-}
270 mice (**Fig.S3e**), while WT mice on HFD displayed a significant higher hepatic fibrosis stage, sinusoidal
271 fibrosis and increased collagen deposition (**Fig.2d-f, Fig.S3f**) compared to the *Msr1*^{-/-} mice. Next, we
272 characterised the livers of HFD-WT and HFD- *Msr1*^{-/-} mice by high-throughput RNA sequencing analysis.
273 The analysis revealed 728 differentially expressed genes (**Table S3**). Gene Ontology analysis of
274 differentially expressed genes highlighted an enrichment for genes correlating to biological processes

275 including “innate immune response”, “phagocytosis” and “lipid metabolic process” (**Fig.2g, Fig.S3g-h**).
276 HFD-*Msr1*^{-/-} mice displayed a reduced hepatic transcript expression of inflammatory cytokines (including
277 *Axl, Ccl6, Il1b, Spp1*), pro-inflammatory immune cell markers (*Ccr5, Cd14, Cd44, S100a8, S100a9*),
278 markers for hepatic stellate cell activation (*Sox9, Pdgfb*) and members of the *Tnfa* signalling pathway
279 (*Ripk3, Tnfaip2, Tnfaip8l2*) when compared with WT mice (**Fig.2g**). Furthermore, *Msr1*^{-/-} mice on HFD
280 showed a shift in gene expression associated with lipid metabolism, with genes including *Acox1, Acox2,*
281 *ApoE, Ces1d, Hsd17b11, Pla2g6* and *Ppara* increasing, and genes such as *Fabp5, Lpcat2, Lpl, Pla2g7* and
282 *Pnpla3* decreasing (**Fig.2g**). Functionally, the measured mitochondrial oxygen consumption rate in viable
283 liver samples of HFD-*Msr1*^{-/-} mice was approximately 50% higher compared to the WT, indicating
284 enhanced metabolic function (**Fig.2h**). Taken together, these results demonstrate that *Msr1* deficiency
285 increases the body weight but protects against features of the metabolic syndrome, including liver
286 inflammation and fibrosis, while modulating hepatic lipid metabolism.

287

288 *Msr1* deficiency prevents formation of pro-inflammatory foamy macrophages in vivo

289 Next, we asked whether the lipid-laden environment is a proximal stimulus leading to *Msr1*-mediated
290 inflammation in the liver and adipose tissue, which may explain the observed metabolic dysfunction. In
291 agreement with our human data, histopathological analysis of the liver and adipose tissue from HFD-fed
292 *Msr1*^{-/-} mice showed no hepatic lipogranuloma and very few foamy macrophages compared to their WT
293 counterparts, demonstrated by F4/80 immunostaining (**Fig.3a**). Moreover, *Msr1*^{-/-} mice displayed lower
294 *Il6* and *Tnfa* serum levels and reduced *Tnfa* and *Il6* gene expression in the liver and eWAT (**Fig.3b-d**).
295 Furthermore, *Msr1* deficiency impaired pro-inflammatory activation of isolated adipose tissue- (ATMs)
296 and hepatic-associated macrophages as shown by lower gene transcripts of *Tnfa* and *Il6* (**Fig.3e-g**).
297 Altogether, these results show that *Msr1* mediates HFD-induced hepatic and adipose tissue
298 inflammation and facilitates macrophage activation toward a pro-inflammatory phenotype.

299

300 *Triggering of Msr1 by lipids induces JNK-mediated pro-inflammatory activation of macrophages*

301 We next investigated the underlying mechanism of *Msr1*-mediated lipid-induced inflammation. We
302 reasoned that *Msr1* is directly responsible for lipid uptake in macrophages, leading to an inflammatory
303 response independent from other cell types. In this regard, we measured the uptake of SFA (palmitic
304 acid, PA) and non-SFA (oleic acid, OA) in *Msr1*^{-/-} and WT bone marrow-derived macrophages (BMDMs)
305 by quantifying Oil-red-O staining using confocal microscopy (**Fig.4a-c, FigS4a**). The analysis revealed that
306 *Msr1* facilitates the uptake of both SFA as well as non-SFA but only SFA induced enhanced levels of *Tnfa*

307 and *Il6* transcripts in BMDMs (**Fig.4d**). Furthermore, blocking of Msr1 receptor with a monoclonal
308 antibody reduced the expression of *Tnfa* and *Il6*, and reduced the phosphorylation of JNK in response to
309 SFA treatment (**Fig.4e-f**). In line with these data, pharmacological inhibition of JNK phosphorylation
310 abrogated the induction of *Tnfa* and *Il6* pro-inflammatory gene expression upon SFA treatment
311 (**Fig.4g-j**). Similarly, using primary *Msr1*^{-/-} hepatic macrophages or WT ones treated with monoclonal
312 antibody resulted in reduced lipid uptake, reduced expression of *Tnfa* and reduced JNK phosphorylation
313 (**Fig.4g-j**). To extend these findings, we co-cultured Hepa1-6 cells with BMDMs or primary hepatocytes
314 with hepatic macrophages which resulted in a comparable response (**Fig.S5a-b**). These data indicate that
315 SFA-induced triggering of Msr1 regulates JNK-mediated pro-inflammatory activation of macrophages in
316 the absence of lipopolysaccharide.

317

318 *Therapeutic inhibition of MSR1 reduces the release of TNFA*

319 To investigate the therapeutic potential of targeting MSR1 in the treatment of NAFLD, we applied an
320 antibody-based intervention using NAFLD mouse models and *ex vivo* human liver slices. WT mice were
321 fed a HFD for 12 weeks and were administered two doses of monoclonal rat anti-mouse Msr1 antibody
322 (n=8 animals) or isotype-matched IgG control (n=9 animals) at week 10 and 11 by intravenous injection.
323 Antibody treatment did not result in any weight difference or changes in glucose or insulin levels at
324 week 12 (**Fig.S6**). Notably, histological assessment did show reduced hepatic fibrosis and sinusoidal/peri-
325 cellular fibrosis in anti-Msr1-treated mice compared to the IgG control mice, while steatosis grade,
326 hepatocyte ballooning and lobular inflammation remained unchanged (**Fig.5a-b**). In addition, F4/80
327 immunostaining showed a reduction in occurrence of hepatic foamy macrophages and lipogranulomas
328 upon treatment, which translated into reduced surface area positivity of F4/80-positive cells (**Fig.5b-c**).
329 Furthermore, treated animals showed reduced expression of *Tnfa* transcript in liver samples and
330 isolated hepatic macrophages (**Fig.5d**).

331 To further investigate whether inhibition of MSR1 prevents the formation of foamy macrophages and
332 release of TNFA in humans, we collected human liver slices with normal morphology from two different
333 patients (2 biological replicates per condition for each patient sample). The samples were incubated
334 with a polyclonal anti-human MSR1 antibody prior to culturing them with a mixture of OA (2mM) and PA
335 (1mM) combined with anti-MSR1 antibody for 16h (**Fig.5e**). Treatment with the antibody reduced the
336 surface area positivity of Kupffer cells as shown by the CD68 immunostaining (**Fig.5f-g**). Moreover, lipid-
337 induced release of TNF- α into the culture medium was reduced upon anti-MSR1 antibody treatment

338 **(Fig.5h)**. Overall, our *in vivo* and *ex vivo* results show that therapeutic inhibition of MSR1 prevents the
339 formation of foamy macrophages and the release of TNF- α .

340

341 Relevance of polymorphisms in *MSR1* region to NAFLD and metabolic traits

342 Next, we asked whether genetic variants in *MSR1* are associated with susceptibility to NAFLD and if
343 there is an association with transcriptional regulatory mechanisms controlling *MSR1* expression. Using
344 previously published genomics data encompassing a cohort of 1,483 European Caucasian patients with
345 histologically proven NAFLD and 17,781 European general-population controls¹³, we identified 4 single
346 nucleotide polymorphisms (SNPs) in or around the *MSR1* locus with p-values $< 5 \times 10^{-4}$, with rs41505344 as
347 the most significant (p = 1.64×10^{-4}) **(Fig.6a and Table S4)**. Quantitative trait analysis for rs41505344 in
348 430,101 patients enrolled in the UKBiobank showed a significant correlation with serum triglycerides
349 and AST levels, even after adjustment for age, gender, BMI, centre, batch and the first ten principal
350 components **(Table 1)**.

351 Our human data indicated that *MSR1* is expressed in the liver on mature endogenous macrophages
352 rather than on infiltrating monocyte-derived macrophages. To unravel transcriptional regulatory
353 mechanisms of *MSR1*, we used publicly available RNA sequencing data comparing human monocytes
354 with differentiated macrophages, which identified 1,208 differentially expressed genes, with *MSR1*
355 mRNA expression increased in the macrophage population.¹⁶ By motif enrichment analysis using
356 iRegulon, we identified eight differentially expressed transcription factors, upregulated in human
357 macrophages compared to monocytes, that are predicted to regulate the expression of *MSR1*: *BHLHE41*,
358 *ETV5*, *HMG3*, *MAF*, *MITF*, *NR1H3*, *THRA* and *ZNF562* **(Fig.6b, Table S5)**. To verify whether these
359 transcription factors bind any regulatory regions near the *MSR1* gene, and in particular the rs41505344
360 SNP locus, we investigated ChIP-sequencing data for these proteins. *MITF*, *MAF*, *THRA* and *NR1H3*
361 proved to bind in the vicinity of the rs41505344 locus, suggesting an indirect role for the SNP in the
362 transcriptional regulation of *MSR1* **(Fig.6c)**. When assessing the rs41505344 genotype in our nanoString
363 cohort, a significant increase in *MSR1* transcript was observed in patients carrying the SNP **(Fig.S7)**.
364 Taken together, these results suggest there is an increased frequency in NAFLD of variants potentially
365 affecting *MSR1* expression during monocyte-macrophage differentiation, which thereby could influence
366 features of obesity-related diseases.

367

368

369 Discussion

370 In this study, we provide evidence that MSR1 is important for the uptake of lipids in macrophages
371 leading to an inflammatory response and metabolic changes throughout the body. In a setting of lipid
372 overload, MSR1 deficiency not only led to reduced hepatic inflammation and changes in hepatic lipid
373 metabolism but it also reduced circulating fatty acids, increased lipid storage in the adipose tissue and
374 improved glucose tolerance, highlighting the importance of the liver-adipose tissue axis in NAFLD and
375 the metabolic syndrome.¹⁷ Our data demonstrated that MSR1 expression was observed in tissue-
376 resident macrophages, the Kupffer cells, rather than in infiltrating monocytes, located in the portal tract,
377 and that the expression increases when differentiating human monocytes towards mature
378 macrophages.^{16, 18} The association between *MSR1* mRNA and disease activity in our study would suggest
379 that there is an ongoing differentiation from infiltrating monocytes towards macrophages during NASH.
380 Although portal inflammation is associated with advanced NAFLD, lobular inflammation has been
381 reported to predict fibrosis progression in human NAFLD, suggesting that disease progression is driven
382 by tissue-resident macrophages rather than infiltrating monocytes.¹⁹ Our results support this as *Msr1*
383 deficiency in HFD-fed mice tempered the lipid-induced inflammatory response in the liver, by reducing
384 the expression of *Axl*, *Il1b*, *S100a8/a9* and *Spp1* but also *Cd44*. *Cd44* expression has been associated
385 with NASH in human and mouse, and is crucial for homing of monocytes into the damaged liver,
386 suggesting that lipid accumulation in tissue-resident macrophages via MSR1 is a trigger to recruit
387 immune cells.²⁰ This is in line with previous reports where it was described that Kupffer cell depletion by
388 clodronate liposomes in mice on a 22 week choline-deficient l-amino acid-defined diet suppresses
389 infiltration of inflammatory cells, mainly monocytes, into the liver.²¹ Furthermore, our results showed
390 that the absence of *Msr1* induced a change in hepatic expression of genes associated with lipid
391 metabolism, including an increase in *Ppara*, with concordantly increased mitochondrial oxygen
392 consumption and ameliorated glucose tolerance in HFD-fed mice. Peroxisome proliferator-activated
393 receptors (PPAR) are nuclear receptors playing key roles in metabolic homeostasis and inflammation.²²
394 Selective Kupffer cell depletion has been reported to activate *Ppara* signalling in hepatocytes while
395 resulting in overall reduced levels of hepatic triglycerides in mice fed a 45%-HFD.²³ Furthermore,
396 hepatocyte-restricted *Ppara* deletion in mice impaired liver lipid metabolism, leading to increased
397 plasma FFAs.²⁴ In human adult non-cirrhotic NASH patients, the pan-PPAR agonist lanifibranor proved to
398 induce NASH resolution after 24 weeks of treatment in a Phase 2b randomised, placebo-controlled,
399 double-blind study.²⁵ Taken together, the effects of *Msr1* deficiency observed in this study on liver

400 metabolism, triglycerides and circulating FFAs could in part be explained by the changed Ppara signalling
401 in the liver.

402 This study showed that MSR1 can facilitate the uptake of SFAs, such as palmitic acid, as well as non-
403 SFAs, such as oleic acid, independent from other receptors. Yet, only SFAs could induce the release of
404 TNF α through phosphorylation of JNK in macrophages, which is in line with previous reports.⁷⁻⁹ In our
405 *Msr1*^{-/-} HFD-fed mice, we observed lower hepatic *Tnfa* expression as well as lower serum Tnfa.
406 Furthermore, therapeutic blocking of MSR1 *in vivo* or *ex vivo* reduced foamy macrophage formation and
407 the release of TNF α . TNF α has a pleiotropic effect as it can sensitise hepatocytes to apoptosis and as it
408 can stimulate hepatic lipid synthesis while reducing *Ppara* expression.^{26,27} Furthermore, *Tnfa* affects
409 glucose homeostasis in adipocytes and promotes lipolysis in cultured adipocytes, and could explain the
410 obese phenotype in our *Msr1*^{-/-} HFD-fed mice.²⁸

411 Although current efforts to develop drug therapies for NAFLD primarily focus on ameliorating the
412 specific histological features of the disease (i.e. steatohepatitis or fibrosis), it is important to remember
413 that NAFLD is part of a multi-system metabolic disease state and so agents that offer more broad
414 metabolic or cardiovascular benefits would be highly attractive. Our data indicate that by targeting
415 MSR1, one would not only reduce lipid-induced inflammation in the liver but also improve dyslipidemia
416 and affect improved lipid storage in the adipocytes. In addition, we demonstrated the feasibility of using
417 targeted monoclonal antibody therapy to treat NASH by reducing hepatic inflammation. Moreover, we
418 found some evidence that the genetic variant rs41505344 in *MSR1* was associated with serum
419 triglycerides and ALT in a large cohort of over 400,000 patients. Though the SNP in *MSR1* was not
420 strongly associated with susceptibility to NAFLD, we found that several transcription factors regulating
421 the expression of *MSR1* bound in the locus and that the SNP was associated with changes in *MSR1*
422 transcript, indicating a role for rs41505344 during macrophage differentiation.

423

424 There are several limitations to this study. We used a global knock-out mouse model and focused on the
425 early phases of NAFLD by using a relative short-term diet of 16 weeks. To further investigate the liver-
426 adipose tissue axis, a Kupffer cell-specific *Msr1* knock-out or a conditional *Msr1* knock-out mouse model
427 challenged to a long term diet would provide more information on advanced NAFLD. Furthermore, we
428 mainly explored the role of SFAs in macrophages, but this does not exclude that exosomes or oxLDL can
429 have an additive effect in the inflammatory response, nor have we explored the synergetic function of
430 other scavenger receptors such as CD36 or TREM2.

431 This study showed that the scavenger receptor MSR1, as part of the innate immune system, is a critical
432 sensor for lipid homeostasis, highlighting the importance of the liver-adipose tissue axis. With the
433 prevalence of obesity increasing globally, it is crucial that we understand how our immune system reacts
434 when challenged with over-nutrition. Understanding and therapeutically influencing macrophage
435 immunometabolism, could help us treat features of the metabolic syndrome, such as dyslipidemia,
436 NAFLD and type II diabetes.

437

438 **Abbreviations:** FFA free fatty acids, NAFL non-alcoholic fatty liver, NAFLD non-alcoholic fatty liver, NASH
439 non-alcoholic steatohepatitis, OA oleic acid, PA palmitic acid, SFA saturated fatty acids, SNP single
440 nucleotide polymorphism

441

442 **Acknowledgments:** The authors would like to thank the Newcastle Bioimaging Unit, the Newcastle
443 University Genomics Core Facility, the Newcastle NanoString Core Facility and the Newcastle Molecular
444 Pathology Node Proximity Laboratory for their technical support.

445

446

447 **References:**

- 448 [1] Anstee QM, Reeves HL, Kotsiliti E, Govaere O, Heikenwalder M. From NASH to HCC: current concepts and
449 future challenges. *Nat Rev Gastroenterol Hepatol* 2019;16:411-428.
- 450 [2] Govaere O, Cockell S, Tiniakos D, Queen R, Younes R, Vacca M, et al. Transcriptomic profiling across the
451 nonalcoholic fatty liver disease spectrum reveals gene signatures for steatohepatitis and fibrosis. *Sci Transl Med*
452 2020;12.
- 453 [3] Krenkel O, Puengel T, Govaere O, Abdallah AT, Mossanen JC, Kohlhepp M, et al. Therapeutic inhibition of
454 inflammatory monocyte recruitment reduces steatohepatitis and liver fibrosis. *Hepatology* 2018;67:1270-1283.
- 455 [4] Kazankov K, Jorgensen SMD, Thomsen KL, Moller HJ, Vilstrup H, George J, et al. The role of macrophages
456 in nonalcoholic fatty liver disease and nonalcoholic steatohepatitis. *Nat Rev Gastroenterol Hepatol* 2019;16:145-
457 159.
- 458 [5] Tiniakos DG, Vos MB, Brunt EM. Nonalcoholic fatty liver disease: pathology and pathogenesis. *Annu Rev*
459 *Pathol* 2010;5:145-171.
- 460 [6] Luukkonen PK, Sadevirta S, Zhou Y, Kayser B, Ali A, Ahonen L, et al. Saturated Fat Is More Metabolically
461 Harmful for the Human Liver Than Unsaturated Fat or Simple Sugars. *Diabetes Care* 2018;41:1732-1739.
- 462 [7] Holzer RG, Park EJ, Li N, Tran H, Chen M, Choi C, et al. Saturated fatty acids induce c-Src clustering within
463 membrane subdomains, leading to JNK activation. *Cell* 2011;147:173-184.
- 464 [8] Lancaster GI, Langley KG, Berglund NA, Kammoun HL, Reibe S, Estevez E, et al. Evidence that TLR4 Is Not a
465 Receptor for Saturated Fatty Acids but Mediates Lipid-Induced Inflammation by Reprogramming Macrophage
466 Metabolism. *Cell Metab* 2018;27:1096-1110 e1095.
- 467 [9] Guo M, Hartlova A, Gierlinski M, Prescott A, Castellvi J, Losa JH, et al. Triggering MSR1 promotes JNK-
468 mediated inflammation in IL-4-activated macrophages. *EMBO J* 2019;38.
- 469 [10] Manning-Tobin JJ, Moore KJ, Seimon TA, Bell SA, Sharuk M, Alvarez-Leite JJ, et al. Loss of SR-A and CD36
470 activity reduces atherosclerotic lesion complexity without abrogating foam cell formation in hyperlipidemic mice.
471 *Arterioscler Thromb Vasc Biol* 2009;29:19-26.
- 472 [11] Bieghs V, Wouters K, van Gorp PJ, Gijbels MJ, de Winther MP, Binder CJ, et al. Role of scavenger receptor
473 A and CD36 in diet-induced nonalcoholic steatohepatitis in hyperlipidemic mice. *Gastroenterology* 2010;138:2477-
474 2486, 2486 e2471-2473.
- 475 [12] Hardy T, Wonders K, Younes R, Aithal GP, Aller R, Allison M, et al. The European NAFLD Registry: A real-
476 world longitudinal cohort study of nonalcoholic fatty liver disease. *Contemp Clin Trials* 2020;98:106175.
- 477 [13] Anstee QM, Darlay R, Cockell S, Meroni M, Govaere O, Tiniakos D, et al. Genome-wide association study
478 of non-alcoholic fatty liver and steatohepatitis in a histologically characterised cohort(). *J Hepatol* 2020;73:505-
479 515.
- 480 [14] Kleiner DE, Brunt EM, Van Natta M, Behling C, Contos MJ, Cummings OW, et al. Design and validation of a
481 histological scoring system for nonalcoholic fatty liver disease. *Hepatology* 2005;41:1313-1321.
- 482 [15] Ramachandran P, Dobie R, Wilson-Kanamori JR, Dora EF, Henderson BEP, Luu NT, et al. Resolving the
483 fibrotic niche of human liver cirrhosis at single-cell level. *Nature* 2019;575:512-518.
- 484 [16] Dong C, Zhao G, Zhong M, Yue Y, Wu L, Xiong S. RNA sequencing and transcriptomal analysis of human
485 monocyte to macrophage differentiation. *Gene* 2013;519:279-287.
- 486 [17] Gastaldelli A, Cusi K. From NASH to diabetes and from diabetes to NASH: Mechanisms and treatment
487 options. *JHEP Rep* 2019;1:312-328.
- 488 [18] Govaere O, Cockell S, Van Haele M, Wouters J, Van Delm W, Van den Eynde K, et al. High-throughput
489 sequencing identifies aetiology-dependent differences in ductular reaction in human chronic liver disease. *J Pathol*
490 2019;248:66-76.
- 491 [19] Brunt EM, Kleiner DE, Wilson LA, Unalp A, Behling CE, Lavine JE, et al. Portal chronic inflammation in
492 nonalcoholic fatty liver disease (NAFLD): a histologic marker of advanced NAFLD-Clinicopathologic correlations
493 from the nonalcoholic steatohepatitis clinical research network. *Hepatology* 2009;49:809-820.
- 494 [20] Patouraux S, Rousseau D, Bonnafous S, Lebeaupin C, Luci C, Canivet CM, et al. CD44 is a key player in non-
495 alcoholic steatohepatitis. *J Hepatol* 2017;67:328-338.
- 496 [21] Miura K, Yang L, van Rooijen N, Ohnishi H, Seki E. Hepatic recruitment of macrophages promotes
497 nonalcoholic steatohepatitis through CCR2. *Am J Physiol Gastrointest Liver Physiol* 2012;302:G1310-1321.

- 498 [22] Francque S, Szabo G, Abdelmalek MF, Byrne CD, Cusi K, Dufour JF, et al. Nonalcoholic steatohepatitis: the
499 role of peroxisome proliferator-activated receptors. *Nat Rev Gastroenterol Hepatol* 2021;18:24-39.
- 500 [23] Stienstra R, Saudale F, Duval C, Keshtkar S, Groener JE, van Rooijen N, et al. Kupffer cells promote hepatic
501 steatosis via interleukin-1beta-dependent suppression of peroxisome proliferator-activated receptor alpha activity.
502 *Hepatology* 2010;51:511-522.
- 503 [24] Montagner A, Polizzi A, Fouche E, Ducheix S, Lippi Y, Lasserre F, et al. Liver PPARalpha is crucial for whole-
504 body fatty acid homeostasis and is protective against NAFLD. *Gut* 2016;65:1202-1214.
- 505 [25] Francque SM, Bedossa P, Ratziu V, Anstee QM, Bugianesi E, Sanyal AJ, et al. A Randomized, Controlled
506 Trial of the Pan-PPAR Agonist Lanifibranor in NASH. *N Engl J Med* 2021;385:1547-1558.
- 507 [26] Faletti L, Peintner L, Neumann S, Sandler S, Grabinger T, Mac Nelly S, et al. TNFalpha sensitizes
508 hepatocytes to FasL-induced apoptosis by NFkappaB-mediated Fas upregulation. *Cell Death Dis* 2018;9:909.
- 509 [27] Beier K, Volkl A, Fahimi HD. TNF-alpha downregulates the peroxisome proliferator activated receptor-
510 alpha and the mRNAs encoding peroxisomal proteins in rat liver. *FEBS Lett* 1997;412:385-387.
- 511 [28] Cawthorn WP, Sethi JK. TNF-alpha and adipocyte biology. *FEBS Lett* 2008;582:117-131.
- 512
- 513

514 **Table 1.** Correlation rs41505344 SNP with clinical features using UK Biobank (n=430,101)
 515

Characteristic	Value	Range	rs41505344_MSR1						Unadjusted	Adjusted for age, gender, BMI, PC 1-10, centre and batch			
			GG		GA		AA			p-value	Inverse normal rank transformation		
			Value	Range	Value	Range	Value	Range			p-value	Beta	CI
n-value	430101		344142		81079		4880						
Age, y (mean ± SD)	56.8±8.03	39-73	56.8±8.03	39-72	56.8±8.02	39-73	56.7±8.06	40-70	0.80				
BMI (mean ± SD)	27.4±4.76	12.1-74.7	27.4±4.77	12.6-68.4	27.4±4.75	12.1-74.7	27.3±4.81	16.2-54.5	0.02				
Male, n (%)	196727 (45.7)		157394 (45.7)		37080 (45.7)		2253 (46.2)		0.80				
ALT (U/L)	23.5±14.1	3.01-495	23.6±14.1	3.1-495	23.5±14.3	3.01-472	23.3±13.1	3.82-286	0.01	0.063	-0.0060		
AST (U/L)	26.2±10.6	3.3-947	26.2±10.5	3.3-947	26.2±11	3.3-711	26±9.72	8.4-227	8.29E-04	0.003	-0.010		
Glucose (mM)	5.12±1.21	1-36.8	5.12±1.2	1.1-36.8	5.12±1.23	1-32.7	5.12±1.18	1.8-22.3	0.76	0.41	0.003		
Cholesterol (mM)	5.71±1.14	0.601-15.5	5.71±1.14	0.601-15.5	5.71±1.14	1.71-13.3	5.68±1.13	2.39-12.3	0.16	0.12	-0.005		
LDL (mM)	3.57±0.87	0.266-9.8	3.57±0.87	0.266-9.8	3.57±0.868	0.751-9.61	3.55±0.862	1.22-7.64	0.16	0.15	-0.0051		
HDL (mM)	1.45±0.382	0.219-4.4	1.45±0.382	0.226-4.4	1.46±0.382	0.219-4.13	1.45±0.38	0.628-3.22	0.03	0.071	0.006		
Triglycerides (mM)	1.75±1.02	0.231-11.3	1.76±1.03	0.233-11.3	1.74±1.02	0.231-11.3	1.72±1	0.375-11	8.27E-07	3.55E-06	-0.015		
Chronic liver disease, n (%)	6024 (1.401)		4807 (1.397)		1161 (1.432)		56 (1.148)		0.98	0.92	1.003	0.946-1.06	
All-cause cirrhosis, n (%)	1709 (0.397)		1349 (0.392)		344 (0.424)		16 (0.328)		0.40	0.37	1.051	0.943-1.17	

516

517

518 **Figure legends**519 **Fig.1. Macrophage Scavenger Receptor 1 (MSR1) expression in human non-alcoholic fatty liver disease**

520 **(NAFLD) correlates with steatosis and steatohepatitis. (a)** mRNA levels of *MSR1* in a cohort of 170
521 histological proven NAFLD samples covering the different stages of the disease using nanoString (Mann-
522 Whitney-U test and Kruskal-Wallis with correction for multiple testing). **(b)** *MSR1* transcript in patients
523 stratified based on $NAS \geq 4$ and presence of NASH (Mann-Whitney-U test). **(c)** Receiver operating
524 characteristic curve showing the binary logistic model based on *MSR1* transcript, MSR1 model,
525 compared to other variables *CD68* transcript, ALT and AST. **(d)** Immunohistochemical analysis of MSR1 in
526 human NAFLD biopsies (n=14), red arrows indicate lipogranuloma and lipid laden macrophages.
527 Histopathological quantification of MSR1 and CD68 immunopositive cells in the parenchyma and portal
528 tract (NAFL n=4; NASH F0-2 n=6; NASH F3-4 n=4; one-way ANOVA or Kruskal-Wallis with correction for
529 multiple testing). **(e)** Differentiation of human monocytes obtained from 5 healthy volunteers towards
530 mature macrophages. MSR1 protein expression was assessed using FACS (n=3, unpaired Student's t-test)
531 and western blotting (n=2). **(f)** Representative image of PLIN2+CD68+ parenchymal macrophages.
532 Quantification was done in a cohort of 10 NAFLD samples (unpaired Student's t-test). Data are
533 presented as mean \pm SEM (* $p < 0.05$, ** $p < 0.01$, *** $p < 0.001$, **** $p < 0.0001$, *ns*: non-significant). Scale
534 bars 100 μ m.

535

536 **Fig.2. Msr1 deficiency protects against HFD-associated metabolic dysregulation and liver damage. (a)**

537 Body weight of *Msr1*^{+/+} (Wild-type, WT) and *Msr1*^{-/-} male aged-matched mice fed high fat/cholesterol
538 diet (HFD) for 16 weeks (n=5 mice/experimental group). **(b)** Epididymal (eWAT) and liver mass of WT
539 and *Msr1*^{-/-} male mice fed with HFD. **(c)** Glucose tolerance test on overnight fasted mice during the 15th
540 week of HFD feeding; AUC (area under curve). **(d)** Histological characterisation of livers specimens from
541 WT and *Msr1*^{-/-} mice fed a HFD for 16 weeks. **(e)** Representative images of morphology of the eWAT and
542 liver from HFD-fed WT and *Msr1*^{-/-} mice. Scale bar 100 μ m. **(f)** Quantification of the adipocyte number
543 per area and hepatic collagen deposition of WT and *Msr1*^{-/-} HFD-fed mice (n = 5 mice/experimental
544 group; Mann-Whitney-U test). **(g)** RNA sequencing data comparing *Msr1*^{-/-} (n=5) with baseline WT (n=4)
545 HFD-fed mice. Gene Ontology enrichment analysis was performed for biological processes and selected
546 differentially expressed genes were visualised with corrected p-values. **(h)** Seahorse analysis of oxygen
547 consumption rates (OCRs) of liver tissue from HFD-fed WT and *Msr1*^{-/-} mice (n = 4/group). Data are
548 presented as mean \pm SEM (unpaired Student's t-test or Mann-Whitney-U test, or one-way ANOVA with

549 correction for multiple testing; p-values are shown for the comparisons WT and *Msr1*^{-/-}; *p < 0.05, **p <
550 0.01, ***p < 0.001, ****p < 0.0001, ns: non-significant).

551

552 **Fig.3. *Msr1* mediates HFD-induced adipose tissue and hepatic inflammation and facilitates**
553 **macrophage activation toward a pro-inflammatory phenotype. (a)** Representative images for F4/80
554 immunostainings in eWAT and liver (scale bars 100µm) from WT and *Msr1*^{-/-} HFD-fed mice
555 (n=5/experimental group). Arrows indicate immunopositive cells. **(b)** Serum levels of Tnfa and Il-6 in NC-
556 and HFD-fed mice (n=5/ group). **(c-d)** Quantification of mRNA levels of *Tnfa*, *Il6* inflammation markers in
557 the eWAT and liver of NC- and HFD-fed mice (n=5/group). **(e-f)** Real-time PCR analysis for markers of
558 inflammation in isolated F4/80⁺ adipose tissue (ATMs) and liver macrophages (n=5 mice/group). Data
559 are presented as mean ± SEM (unpaired Student's t-test or Mann-Whitney-U test, or one-way ANOVA or
560 Kruskal-Wallis with correction for multiple testing; p-values are shown for the comparisons WT and
561 *Msr1*^{-/-}; *p < 0.05, **p < 0.01, ***p < 0.001, ****p < 0.0001, ns: non-significant).

562

563 **Fig.4. *Msr1* regulates JNK-mediated lipid-induced pro-inflammatory activation of macrophages. (a)**
564 Representative image of lipid uptake (mixture of 1mM Palmitic acid, saturated fatty acids (SFA), and
565 2mM Oleic, non-saturated fatty acids (non-SFA)) by WT and *Msr1*^{-/-} bone marrow derived macrophages
566 (BMDMs) visualised by Oil-red-O staining using confocal microscopy (n=3). **(b-c)** Quantification of SFA
567 (palmitic acid 1mM) and non-SFA (oleic acid 2mM) uptake in WT and *Msr1*^{-/-} BMDMs, or WT BMDMs
568 pre-treated with or without anti-*Msr1* antibody (n=5). Data are normalised to the average of the WT
569 BMDM group. **(d)** Real-time PCR analysis for *Tnfa* and *Il6* in WT and *Msr1*^{-/-} BMDMs stimulated or not
570 either with SFA, non-SFA or bovine serum albumin (BSA) control for 6 hrs. **(e)** Real-time PCR analysis of
571 BMDMs with or without SFA stimulation that were treated with 10 or 25µg/ml anti-*Msr1* monoclonal
572 antibody for 6 hrs. **(f)** Flow cytometry analysis and quantification of JNK1/2 phosphorylation in WT and
573 *Msr1*^{-/-} BMDMs stimulated with SFA or BSA control. **(g)** Quantification of SFA and non-SFA uptake in WT
574 and *Msr1*^{-/-} primary liver macrophages (n=3). Data are normalised to the average of the WT BMDM
575 group. **(h)** Real time-PCR analysis and **(i)** flow cytometry analysis of phospho-JNK (Thr183/Tyr185) in WT
576 and *Msr1*^{-/-} primary liver macrophages treated either with control BSA or SFA or non-SFA for 6hrs (n=3).
577 **(j)** Real time-PCR analysis of WT primary liver macrophages treated with or without monoclonal anti-
578 *Msr1* antibody (n=3). Data are shown as mean ± SEM (unpaired Student's t-test or one-way
579 ANOVA/Kruskal-Wallis with correction for multiple testing; for panels d and f-i the p-values are shown

580 only for grouped comparisons per experimental condition; * $p < 0.05$, ** $p < 0.01$, *** $p < 0.001$, **** $p <$
581 0.0001).

582

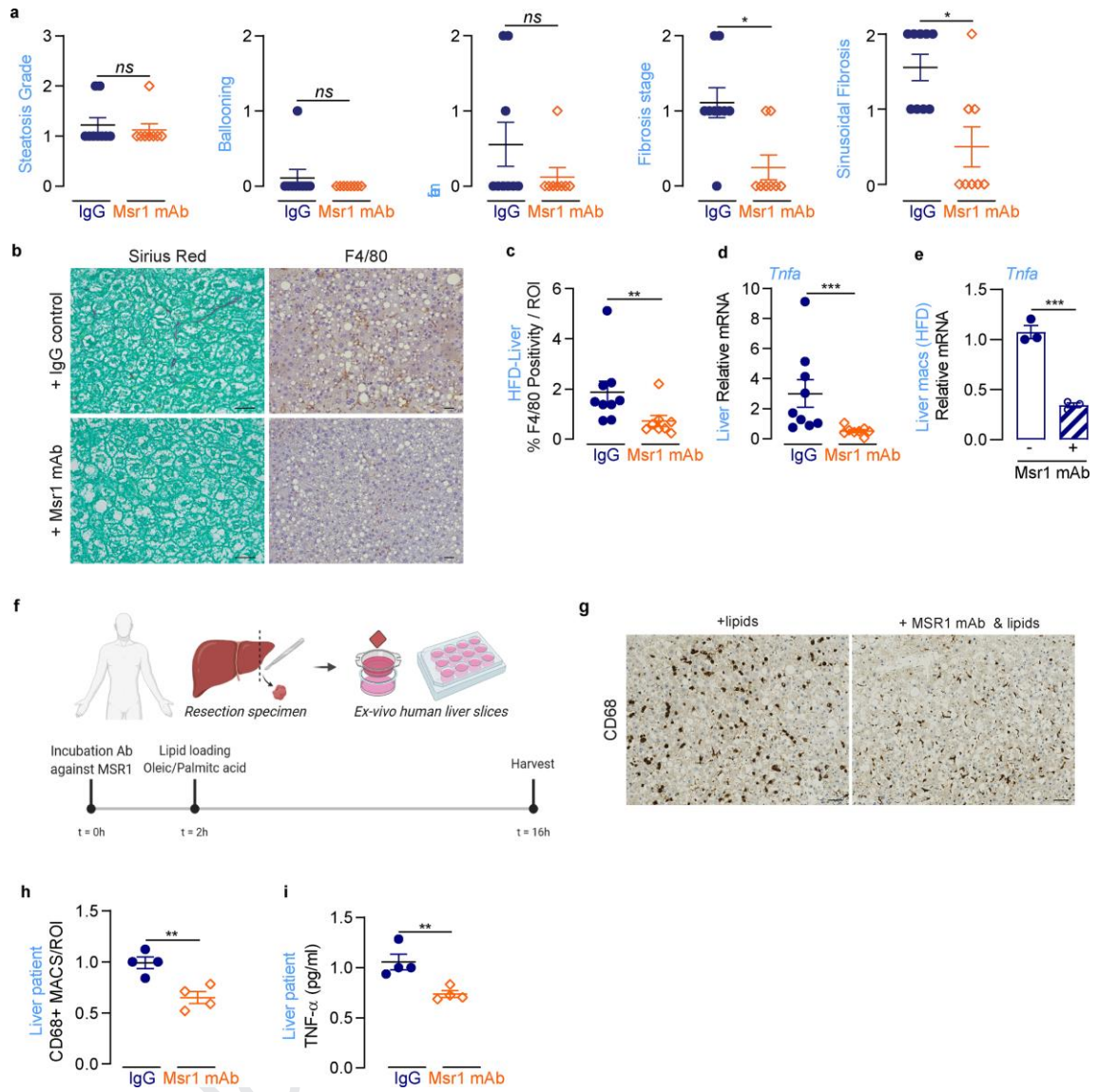
583 **Fig.5. Therapeutic inhibition of MSR1 prevents formation of pro-inflammatory foamy macrophages.**

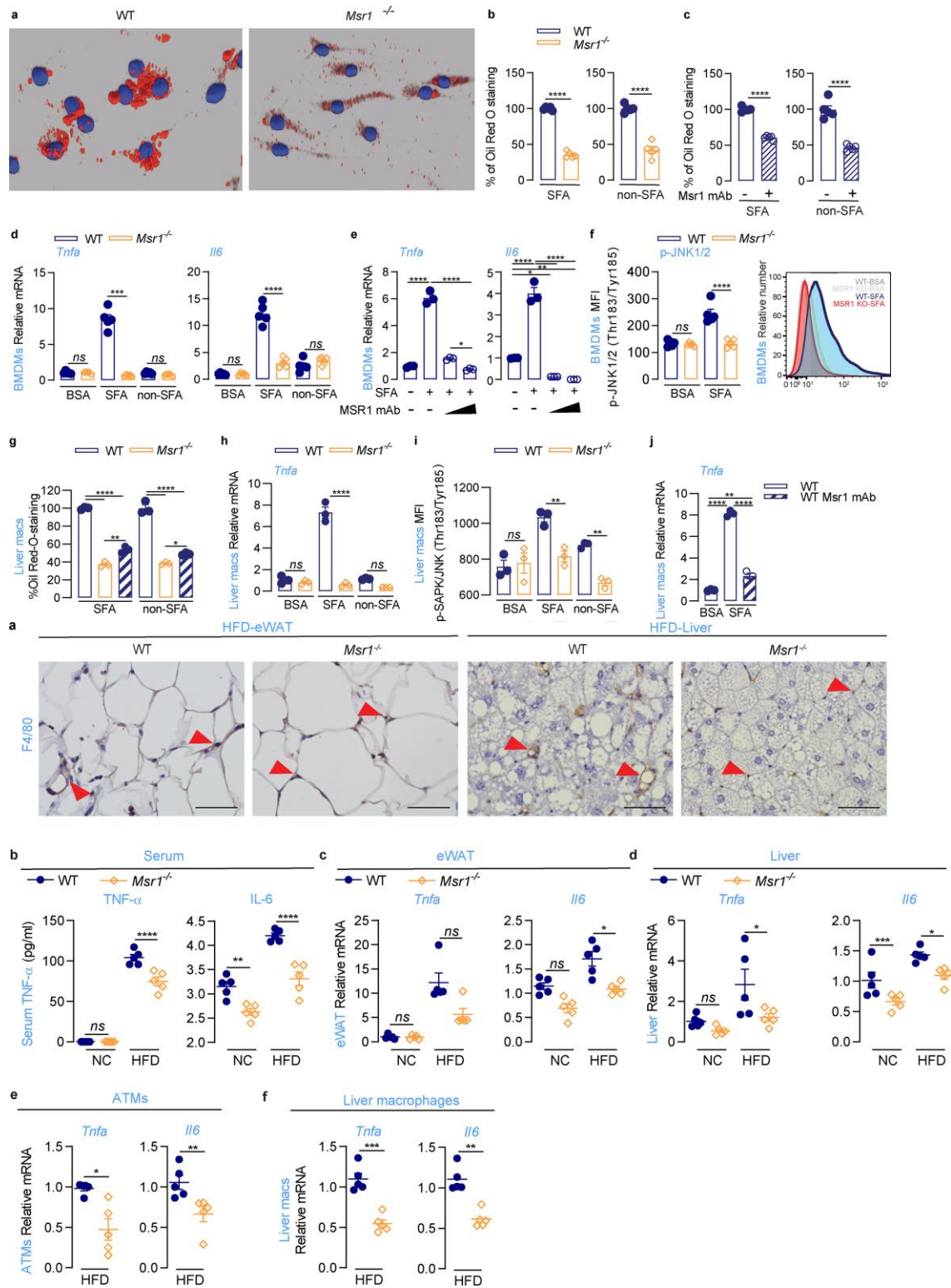
584 (a) Histological characterisation of livers specimens from WT male mice fed a HFD for 12 weeks and
585 treated with anti-Msr1 antibody (n=8) or IgG control (n=9) at week 10 and 11. (b) Representative images
586 of morphology of HFD-fed animals treated with anti-Msr1 antibody or IgG control. (c) Quantification of
587 F4/80 staining from treated animals presented as percentage pixel positivity of the region of interest
588 (ROI). (d-e) Real-time PCR analysis for *Tnfa* transcript in liver samples and isolated hepatic macrophages
589 from HFD-fed animals treated with anti-Msr1 antibody (n=8) or IgG control (n=9). Isolated primary liver
590 macrophages were pooled together before real-time PCR analysis (n=3). (f) Schematic overview of
591 antibody-based treatment of *ex vivo* lipid-loaded human liver slices. Samples were loaded with a
592 combination of oleic (2mM) and palmitic acid (1mM). (g) Immunohistochemical staining for CD68 on
593 human lipid-loaded liver slices treated with or without anti-MSR1 antibody. (h) Quantification of CD68
594 staining presented as percentage pixel positivity of the region of interest (ROI). Normalisation was done
595 to untreated reference. (i) TNF- α ELISA from human liver slices treated with lipids or anti-MSR1-
596 antibody+lipids. Data are presented as mean \pm SEM (unpaired Student's t-test or Mann-Whitney-U test;
597 * $p < 0.05$, ** $p < 0.01$, *** $p < 0.001$). Scale bars 50 μ m.

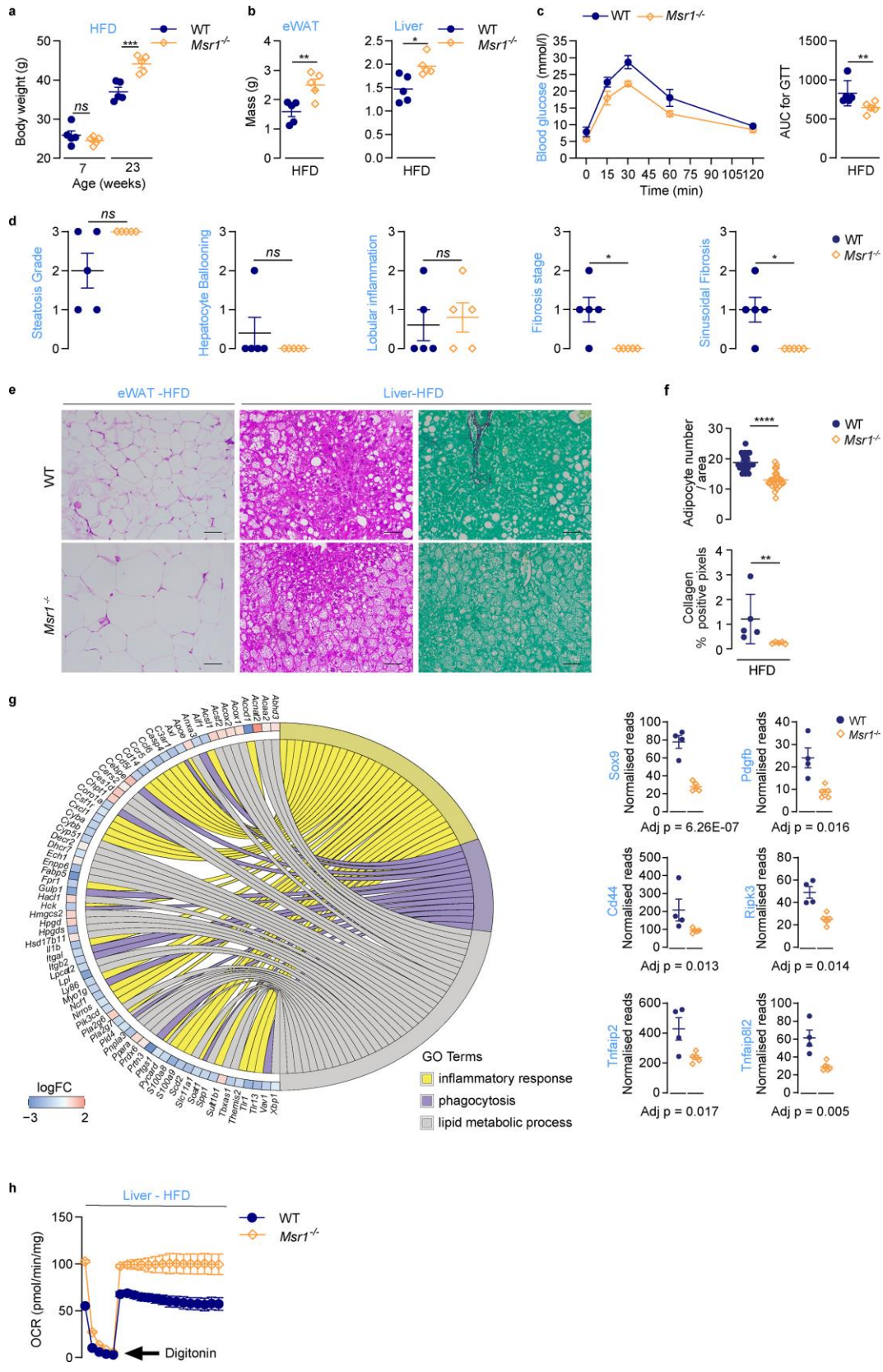
598

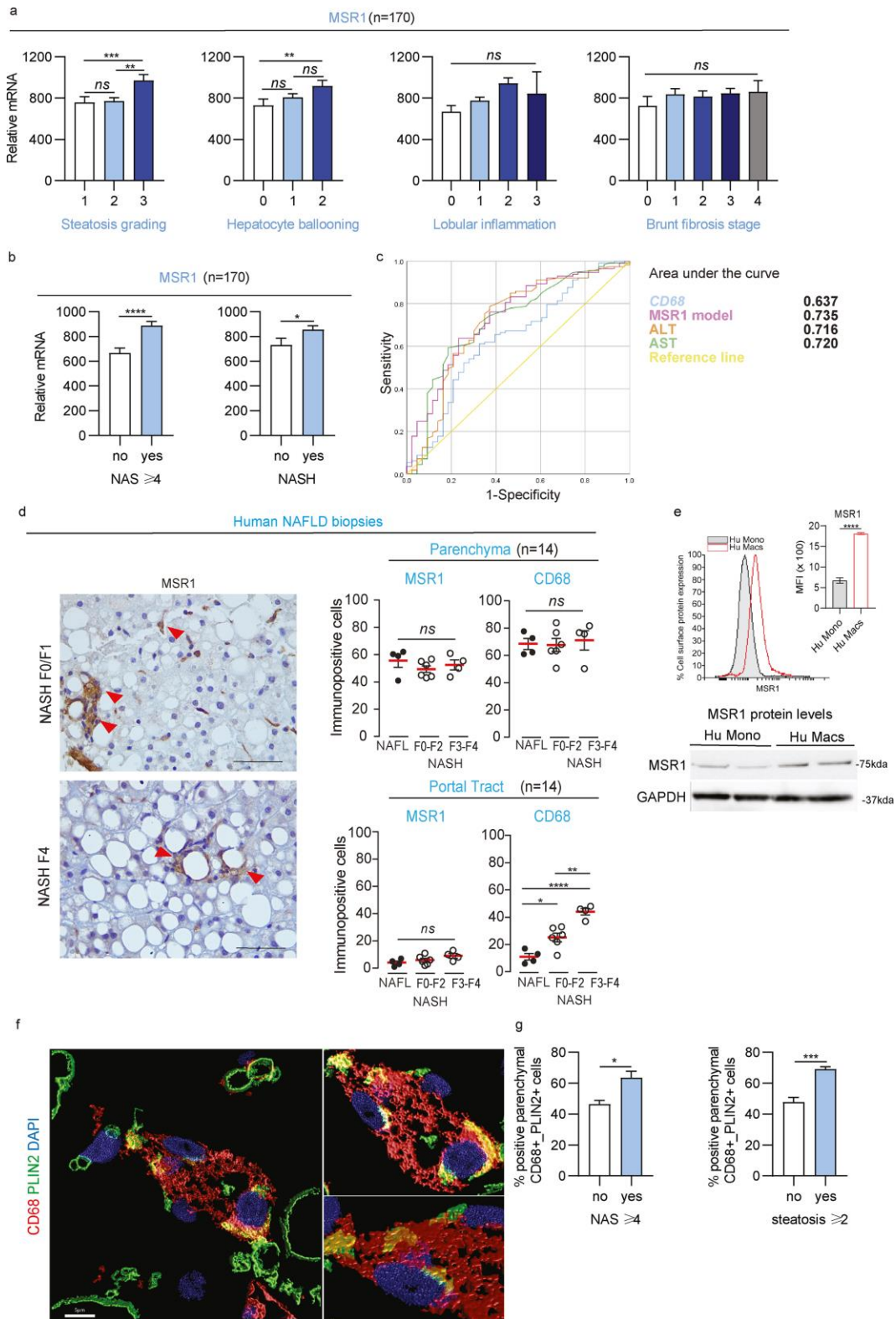
599 **Fig.6. Regulatory mechanisms of MSR1 expression in human NAFLD.**

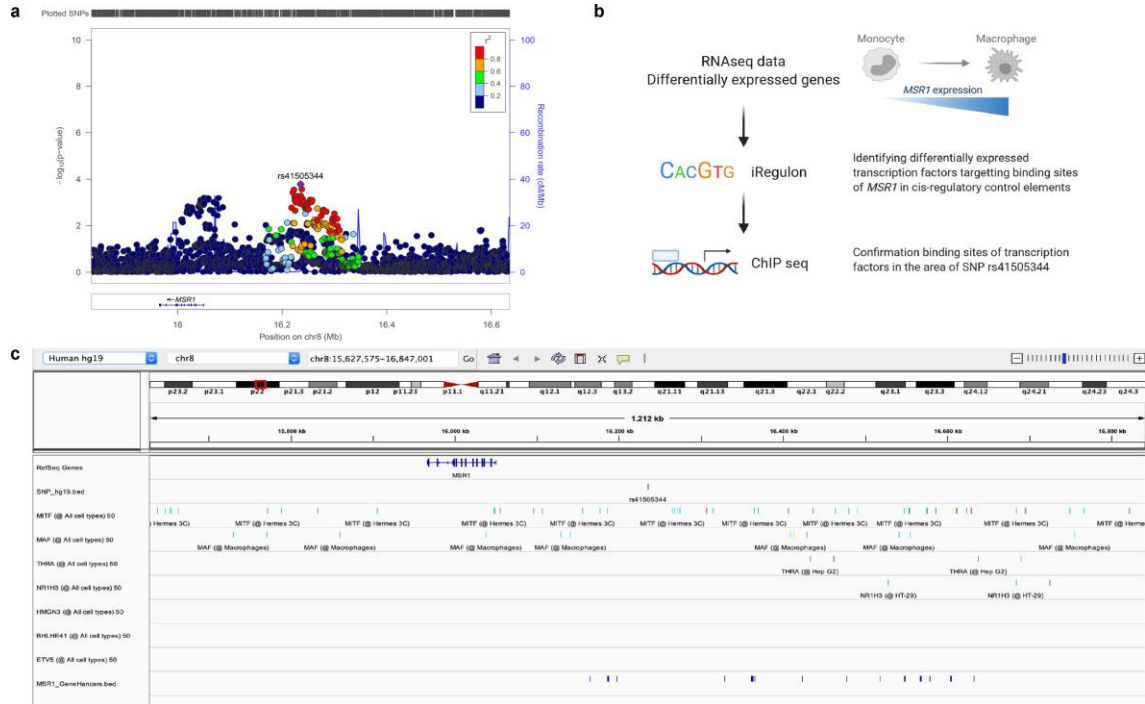
600 (a) Locus plot showing *MSR1* rs41505344 SNP based on case-control analysis comparing 1,483
601 histologically characterised NAFLD samples with 17,781 matched population controls. (b) Schematic
602 overview of the workflow used to identify transcriptional regulatory mechanisms of *MSR1* from publicly
603 available RNA sequencing data, comparing human monocytes with differentiated macrophages.¹⁶ (c)
604 Visualisation of chromatin immunoprecipitation sequencing data around *MSR1* rs41505344 SNP of the
605 predicted transcription factors that are differentially expressed in the RNA sequencing data as identified
606 by iRegulon. Bottom row indicates known transcriptional regulatory regions of *MSR1*.











Journal Pre-proof

Highlights

- In human NAFLD, MSR1 is expressed in mature Kupffer cells and foamy macrophages
- *MSR1* transcript levels are associated with disease activity in patients with NAFLD
- Mice lacking *Msr1* are protected against diet-induced metabolic disorder
- MSR1 is essential for the uptake of lipids in mature macrophages
- Uptake of saturated fatty acids via MSR1 results in a pro-inflammatory response
- The SNP rs41505344 upstream of MSR1 is associated with altered serum triglycerides